Efficacy of Radioembolization with ^{166}Ho-Microspheres in Salvage Patients with Liver Metastases: A Phase 2 Study

Jip F. Prince[1], Maurice A.A.J. van den Bosch[1], Johannes F.W. Nijsen[1], Maarten L.J. Smits[1], Andor F. van den Hoven[1], Stavros Nikolakopoulos[2], Frank J. Wessels[1], Rutger C.G. Bruijnen[1], Manon N.G.J.A. Braat[1], Bernard A. Zonnenberg[1], and Marnix G.E.H. Lam[1]

[1]*Department of Radiology and Nuclear Medicine, University Medical Center Utrecht, Utrecht, The Netherlands; and* [2]*Department of Biostatistics, Julius Center for Health Sciences and Primary Care, University Medical Center Utrecht, Utrecht, The Netherlands*

Radioembolization of liver malignancies with ^{166}Ho-microspheres has been shown to be safe in a phase 1 dose-escalation study. The purpose of this study was to investigate the efficacy of ^{166}Ho radioembolization. **Methods:** In this prospective single-arm study, 56 patients were enrolled, all with liver metastases refractory to systemic therapy and ineligible for surgical resection. The primary outcome was a response by 2 target lesions on triphasic liver CT scans 3 mo after therapy, as assessed using RECIST, version 1.1. Secondary outcomes included overall tumor response, time to imaging progression, overall survival, toxicity, quality of life, and quantification of the microspheres on SPECT and MRI. **Results:** Between May 2012 and March 2015, 38 eligible patients were treated, one of whom was not evaluable. In 27 (73%) of 37 patients, the target lesions showed complete response, partial response, or stable disease (disease control) at 3 mo (95% confidence interval [CI], 57%–85%). The median overall survival was 14.5 mo (95% CI, 8.6–22.8 mo). For colorectal cancer patients (n = 23), the median overall survival was 13.4 mo (95% CI, 8.2–15.7 mo). Grade 3 or 4 toxic events after treatment (according to the Common Terminology Criteria for Adverse Events, version 4.03) included abdominal pain (in 18% of patients), nausea (8%), ascites (3%), fatigue (3%), gastric stenosis (3%), hepatic failure (3%), liver abscesses (3%), paroxysmal atrial tachycardia (3%), thoracic pain (3%), upper gastrointestinal hemorrhage (3%), and vomiting (3%). On SPECT, ^{166}Ho could be quantified with high accuracy and precision, with a mean overestimation of 9.3% ± 7.1% in the liver. **Conclusion:** Radioembolization with ^{166}Ho-microspheres induced a tumor response with an acceptable toxicity profile in salvage patients with liver metastases.

Key Words: gastrointestinal; radionuclide therapy; radioembolization; SIRT; holmium; liver

J Nucl Med 2018; 59:582–588
DOI: 10.2967/jnumed.117.197194

Hepatic radioembolization involves the injection of radioactive microspheres into the hepatic arteries, with the aim of embolizing and irradiating liver malignancies. The microspheres most often used contain the radioactive isotope ^{90}Y, which can be quantified on bremsstrahlung SPECT/CT or PET/CT, but only after a full treatment dose (*1*). Pretreatment imaging can be performed with ^{99m}Tc-macroaggregated albumin (^{99m}Tc-MAA) (*2–4*). Microspheres containing ^{166}Ho emit γ-rays (81 keV) and can be visualized on SPECT/CT with high sensitivity, enabling quantification at lower activities such as after a scout dose (*5*). A scout dose with ^{166}Ho-microspheres enables individualized treatment dosimetry (*6,7*).

A previous phase 1 dose-escalation study showed that ^{166}Ho radioembolization, with a projected average absorbed dose of up to 60 Gy to the liver, was safe (*8*). In this phase 2 study, the efficacy was investigated.

MATERIALS AND METHODS

Study Design

The Holmium Embolization Particles for Arterial Radiotherapy II study was a single-arm, single-center study (Clinicaltrials.gov identifier NCT01612325).

Patients were eligible if diagnosed with metastatic liver lesions of any primary origin and limited disease outside the liver as determined on ^{18}F-FDG PET/CT (the sum of lesion diameters had to be <50% of the sum of lesions inside the liver); were unable or unwilling to undergo (further) chemotherapy or surgery (salvage patients); had an estimated life expectancy of more than 3 mo; had adequate liver, renal, and bone marrow function; and had a World Health Organization performance score of no more than 2. The study protocol was described previously and can be found in a Zenodo repository (*9*).

The study was conducted in accordance with the Declaration of Helsinki and was approved by the local research ethics committee. All patients provided written informed consent. An independent monitor verified all data. All data mentioned in this article are available on request (imaging_research@umcutrecht.nl).

Microspheres

Nonradioactive ^{165}Ho-microspheres were manufactured at University Medical Center Utrecht, neutron-irradiated to obtain radioactive ^{166}Ho-microspheres (Reactor Institute Delft), and subsequently dispersed in water for injection containing 2% Pluronic F-68 (BASF Corp.) and 10% absolute ethanol as described previously (*10*). After 8 patients had been treated, ethanol was replaced by an isotonic phosphate buffer (116 mM, pH 7.4) to improve the microsphere stability, and additional quality controls were implemented.

Treatment

Preparatory angiography was performed at a median of 7 d (range, 2–21 d) before treatment. Extrahepatic vessels (gastroduodenal, right gastric, or pancreatic arteries) were coil-embolized if distal or near the injection positions. Tumor-feeding arteries (phrenic or segmental

Received Jun. 8, 2017; revision accepted Sep. 5, 2017.
For correspondence or reprints contact: Jip F. Prince, Department of Radiology and Nuclear Medicine, UMC Utrecht, E 01.132, P.O. Box 85500, 3508 GA Utrecht, The Netherlands.
E-mail: jipfprince@gmail.com
Published online Sep. 15, 2017.

hepatic arteries, such as from the left gastric artery) were coil-embolized if necessary. A scout dose of ^{99m}Tc-MAA (150 MBq, Technescan LyoMAA; Mallinckrodt Medical B.V.) was administered to assess the safety of subsequent administrations. If more than 20% of the particles shunted to the lungs, treatment was cancelled. On the day of treatment, ^{166}Ho-microspheres were administered first as a scout dose (aimed ^{166}Ho activity of 250 MBq, 60 mg, 0.04 mL, 3 million microspheres) and second as a treatment dose (variable ^{166}Ho activity, 0.54 g, 0.39 mL, 30 million microspheres), with SPECT/CT and MR image acquisition after both injections. Treatment was planned as a single session unless there were more than 3 injection positions. The total amount of radioactivity was adjusted to the targeted liver mass measured on CT (aimed absorbed dose, 60 Gy or 3.8 GBq/kg of liver tissue, including the ^{166}Ho scout dose) and was contained in a fixed number of microspheres. The prepared activities exceeded the prescribed activities by around 10% to account for losses during preparation and administration. Before treatment, patients received proton pump inhibitors (pantoprazole, 40 mg for 6 wk), antiemetics (ondansetron, 8 mg intravenously), and steroids.

Assessments

The primary outcome was the disease control rate of target lesions after 3 mo according to RECIST, version 1.1, on triphasic liver CT (*11*). Secondary outcomes included overall tumor response, response on ^{18}F-FDG PET/CT (not presented here), time to imaging progression, overall survival, toxicity, quality of life, and quantification of the microspheres on SPECT and MRI.

After treatment, follow-up included visits after 3, 6, and 9 wk and then every 3 mo. Response imaging was performed every 3 mo using triphasic liver CT and ^{18}F-FDG PET/CT. Patients were followed until intrahepatic progressive disease occurred, with a maximum of 12 mo.

Three independent readers scored the primary outcome. The outcome was determined by the majority vote ($\geq$2) or considered "not evaluable" (e.g., when all reviewers had a different outcome). Response was dichotomized into progression or disease control, that is, complete response, partial response, or stable disease. For a conservative estimation, progressive disease was inferred if patients were not evaluable, if data were missing at random, or if data were missing not at random (definitions can be found in Sterne et al. (*12*)). Only if data were missing completely at random did we enter the data as not available.

Adverse events were registered and laboratory tests performed at every visit and graded according to the Common Terminology Criteria for Adverse Events (CTCAE), version 4.03, of the National Cancer Institute (*13*). The maximum severity of adverse events after treatment was reported. Quality of life was assessed using the European Organization for Research and Treatment of Cancer score and liver metastasis questionnaires at baseline, 6 wk, and every 3 mo. After 11 patients had been treated, an extra questionnaire 1 wk after treatment was added to better reflect patients' transient symptoms.

^{166}Ho-microspheres were quantified on SPECT/CT with in-house–developed Monte Carlo reconstructions (Utrecht Monte Carlo System), using in-house–developed software (Volumetool) (*5,14*). MR quantification was based on the impact of ^{166}Ho on T2* relaxation times, using multigradient echo sequences and performed on in-house–developed software, similar to earlier reports (*15,16*) but using adjusted acquisition parameters. Both quantifications were compared with the injected number of microspheres (corrected for residual microspheres). Prepared and residual radioactivity values were obtained from a dose calibrator (assumed uncertainty, 10%) (VDC-404; Veenstra Instruments) (*5*).

SPECT/CT (5,6). SPECT/CT was performed on a Symbia T16 system (Siemens Healthcare). For ^{99m}Tc-MAA, low-energy high-resolution collimators were used. Planar scintigraphy was performed during 300 s with a photopeak window of 140 keV $\pm$7.5% (matrix, 256 $\times$ 256; zoom, 1.0; pixel size, 2.4 $\times$ 2.4 mm). A ^{57}Co flood source was used to delineate the lungs. For ^{166}Ho, medium-energy collimators were used. SPECT was performed during 60 min (120 angles, 30 s per projection) with a photopeak window of 81 keV $\pm$ 7.5% over a 360° orbit (noncircular). A low-dose CT scan was acquired on the same scanner for attenuation correction and fusion (16-slice; 110 kVp; adaptive dose modulation; effective mAs, 30). The Utrecht Monte Carlo System software was used to reconstruct SPECT images (isotropic voxels, 4.8 mm).

MRI (6,15). MRI was performed on a 1.5-T whole-body system (Achieva; Philips Healthcare) equipped with a 16-element torso coil. For detection and quantification of ^{166}Ho-loaded poly(L-lactic acid) microspheres, a multislice multigradient echo sequence was used, sampling both the free induction decay and the spin echo envelope. For the data presented in this paper, only the free-induction-decay readout was used for quantification. The spin echo data were acquired for testing a new quantification method that is not included in this paper. Eleven gradient echoes of the free induction decay were acquired during breath-hold with an in-plane resolution of 2 $\times$ 2 $\times$ 2 mm and a slice thickness of 6 mm. Imaging parameters included a 344 $\times$ 384 mm field of view; 45 slices; a repetition time, first echo time, and change in echo time of 360, 3.08, and 0.83 ms, respectively; and a 90° flip angle. Sensitivity encoding with a factor of 4.3 was used for acceleration, resulting in an imaging time of 5 $\times$ 20 s during breath-hold.

Statistical Analysis

For efficacy, an exact group-sequence design was used to define stopping boundaries beforehand. The design had an exact type I error of 4.5% (1-sided) if the true disease control rate was 20%, and power of 90% if the true disease control rate was 40%. Futility boundaries were also used so that the study could be stopped if the disease control rate was considerably lower than the 40% projected by the power calculation (*17*). We aimed to include 30–48 patients with interim analyses scheduled when the primary outcome became available for 30, 36, and 42 patients. The stopping boundaries after analysis of the first 30 patients were 5 (for futility) and 11 (for efficacy) (Supplemental Fig. 1 shows all boundaries; supplemental materials are available at http://jnm.snmjournals.org). Inclusion continued while we were awaiting the first patients to reach the time of the first follow-up.

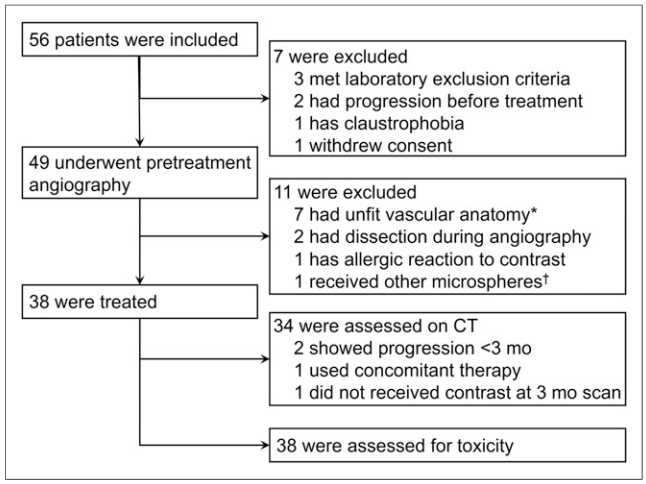

FIGURE 1. Flowchart of study. *Metastases could not be adequately targeted, extrahepatic tissue was also targeted, or there were more than 3 injection positions. †Laboratory experiments indicated need to optimize microsphere production process; treatments were halted until optimization was complete.

TABLE 1
Baseline Characteristics of Treated Patients (n = 38)

Characteristic	Value
Age (y)	66 (41–84)
Sex	
Male	22 (58%)
Female	16 (42%)
World Health Organization performance status	
0	32 (84%)
1	5 (13%)
2	1 (3%)
Primary malignancy	
Colorectal	23 (61%)
Breast	4 (11%)
Cholangiocarcinoma	4 (11%)
Neuroendocrine tumor	2 (5%)
Uveal melanoma	2 (5%)
Pancreatic cancer, gastric cancer, or thymoma	3 (8%)
Time since diagnosis (mo)	28 (4–95)
Occurrence of liver metastases	
Synchronous	19 (50%)
Metachronous	19 (50%)
Time since liver metastases (mo)	18 (3–92)
Extrahepatic disease on ^{18}F-FDG PET/CT	
Lung	8/10 (80%)
Lymph node	4/10 (40%)
Skeletal	2/10 (20%)
Liver mass (kg)	2.0 (1.2–4.0)
Tumor load on contrast-enhanced CT	
0%–25%	30 (79%)
25%–50%	6 (16%)
>50%	2 (5%)

Qualitative data are expressed as numbers followed by percentages in parentheses; continuous data are expressed as median followed by range in parentheses.

Evaluation of toxicity used a continuous sequential analysis based on the expectation of severe toxicity events in 25% of patients, a limit of severe toxicity events in 50% of patients, and a type I error of no more than 5% (1-sided) (*18*). Severe toxicity was defined as all CTCAE events of grade 3 or higher and all serious adverse events as defined by the local research ethics committee, but only if they were not caused by baseline concomitant disease, intercurrent disease, or disease progression. Safety was monitored every 3 mo both by an independent data monitoring committee and by the Dutch Health Care Inspectorate (Inspectie voor de Gezondheidszorg).

Descriptive statistics were calculated as median and range, median and interquartile range, mean and SD, or percentage and frequency. Patients were followed until January 20, 2016. Analyses for survival and time to progression were performed by the Kaplan–Meier method on a per-protocol set. Differences between groups were tested using the log-rank test. Survival was measured from administration of ^{166}Ho-microspheres to either end of follow-up or death. The 95% confidence intervals (CIs) for proportions (e.g., of response data) were displayed as adjusted Wald intervals (*19*). Two-sided P values were calculated (with the exception of the efficacy analysis). Analyses were performed using R statistical software (version 3.2.1 for Microsoft Windows).

RESULTS

Patients

From May 2012 until March 2015, 56 patients were enrolled, 38 of whom received treatment with ^{166}Ho-microspheres (Fig. 1). Of

TABLE 2
Treatment Characteristics of Colorectal Cancer Patients (n = 23)

Characteristic	Value
Chemotherapy (prior to study inclusion)	
Total	23 (100%)
Capecitabine	22 (96%)
Oxaliplatin	21 (91%)
Bevacizumab	14 (61%)
Irinotecan	11 (48%)
5-fluorouracil	6 (26%)
Leucovorin	5 (22%)
Panitumumab	4 (17%)
Cetuximab	1 (4%)
Dabrafenib	1 (4%)
Tegafur-uracil	1 (4%)
Targeted part of liver	
Whole liver	36 (95%)
Right lobe	2 (5%)
Left lobe	0 (0%)
Treatment sessions	
1	36 (95%)
2	2 (5%)
Specific activity (MBq/mg)*	11.26 (4.95–21.34)
Infused activity (MBq)*	6,412 (2,213–13,189)
Administration of treatment dose†	96% (41%–99%)
Adequate administration of activity (>90%)‡	26/37 (70%)
Absorbed liver dose (Gy)	51 (26–69)
Predicted lung shunt (^{99m}Tc-MAA)	3.2% (0.01%–19.3%)
Actual lung shunt (^{166}Ho)	0.02% (0%–0.7%)

*All injections combined (including scout dose), at respective time of injection.

†Percentage of prepared.

‡In other patients, stasis occurred or infusion was stopped because of pain.

Qualitative data are expressed as numbers followed by percentages in parentheses; continuous data are expressed as median followed by range in parentheses.

TABLE 3
Response on Contrast-Enhanced CT

Response category	Target lesions	Liver-specific	Abdomen
3 mo			
Complete response	—	—	—
Partial response	5 (14)	5 (14)	5 (14)
Stable disease	22 (59)	13 (35)	9 (24)
Progressive disease*	10 (27)	19 (51)	23 (62)
Total	37 (100)	37 (100)	37 (100)
6 mo			
Complete response	1 (3)	1 (3)	1 (3)
Partial response	2 (5)	2 (5)	2 (5)
Stable disease	10 (26)	4 (11)	3 (8)
Progressive disease*	25 (66)	31 (82)	32 (84)
Total	38 (100)	38 (100)	38 (100)
9 mo			
Complete response	1 (3)	1 (3)	1 (3)
Partial response	1 (3)	—	—
Stable disease	2 (5)	1 (3)	1 (3)
Progressive disease*	34 (89)	36 (95)	36 (95)
Total	38 (100)	38 (100)	38 (100)
12 mo			
Complete response	—	—	—
Partial response	—	—	—
Stable disease	2 (5)	—	—
Progressive disease*	36 (95)	38 (100)	38 (100)
Total	38 (100)	38 (100)	38 (100)

*Not evaluable, or disease progression was inferred for patients with missing data.

Data are *n* followed by percentage in parentheses. Timing was at median of 90 d (range, 76–104 d) after treatment at 3 mo, 181 d (152–195) at 6 mo, 278 d (252–312) at 9 mo, and 369 d (368–369) at 12 mo.

the treated patients, 23 (61%) had colorectal cancer. Overall, the study population had been diagnosed with a malignancy a median of 28 mo beforehand (range, 4–95 mo) and with liver metastases a median of 18 mo beforehand (range, 3–92 mo; Table 1).

Treatment and Efficacy

Of 38 patients, 2 were treated in 2 separate sessions for both liver lobes (both 3 wk later with a target absorbed dose of 60 Gy for both the right and left liver lobes). Two other patients received right lobar treatment, and the remaining patients received whole-liver treatment in 1 session. The median absorbed dose to the liver was 51 Gy (range, 26–69 Gy, Table 2).

At the first interim analysis, the stopping boundary for efficacy was surpassed and study inclusion was stopped. One patient was not evaluable because intravenous contrast was not used during the CT acquisition at 3 mo. Of the 37 evaluable patients, 2 patients had clinical progressive disease before 3 mo, and in 1 patient progressive disease was inferred because of a protocol deviation (namely, concomitant treatment within 3 mo). All other patients were evaluable at 3 mo as planned.

The target lesions showed disease control on CT imaging in 27 (73%) of the 37 evaluable patients after 3 mo (95% CI, 57%–85%; Table 3). The proportion of specific agreement between the 3 readers was 88% for the assessment of disease control or progression of target lesions at 3 mo after treatment. Disease control in the liver (assessing also new lesions and progression of nontarget lesions) was achieved in 18 (49%) of 37 patients (95% CI, 33%–64%) after 3 mo. The median time to progression in the liver was 3 mo (95% CI, 3–6 mo; Supplemental Fig. 2).

The median overall survival was 14.5 mo (95% CI, 8.6–22.8 mo; Supplemental Fig. 3A). The overall survival analysis was based on 29 deaths (76%) after a median follow-up of 13.3 mo (range, 2.5–39.3 mo). Ten (45%) of 22 colorectal cancer patients showed whole-liver disease control on CT imaging after 3 mo (95% CI, 27%–65%) (1 patient did not receive intravenous contrast medium). Their median overall survival was 13.4 mo (95% CI, 8.2–15.7 mo; Supplemental Fig. 3B). The median overall survival of colorectal cancer patients with disease control of their target lesions after 3 mo was 14.1 mo (95% CI, 8.2 mo–∞). Colorectal cancer patients with progression of their target lesions had a median survival of 7.1 mo (95% CI, 3.3 mo–∞ [$P = 0.44$]; Fig. 2).

Toxicity

The continuous interim analysis showed an acceptable toxicity profile, with 10 (26%) of 38 patients (95% CI, 25%–42%) experiencing severe toxicity as defined in the protocol (i.e., related to therapy and either CTCAE ≥ grade 3 or a serious adverse event). The most common adverse events during follow-up were gastrointestinal complaints as part of the postradioembolization syndrome: nausea, abdominal pain, and fatigue (Tables 4 and 5).

Two deaths occurred within 3 mo after treatment. One patient had a rapid recurrence of gastric cancer that compromised oral intake.

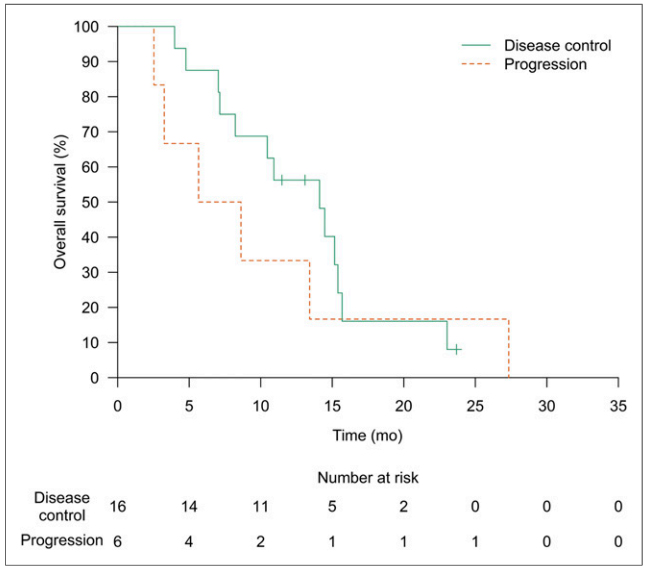

FIGURE 2. Kaplan–Meier estimate of median overall survival was 14.1 mo (95% CI, 8.2 mo–∞) for patients with colorectal disease and disease control of target lesions at 3 mo, and 7.1 mo (95% CI, 3.3 mo–∞) for patients with progressive target lesions at 3 mo ($P = 0.44$). Data of 1 patient are missing (Fig. 1).

TABLE 4
Adverse Events—Clinical

Adverse event	Any time	≤1 wk	>1 wk	Grade 3 or 4
Nausea	74% (28)	71% (27)	34% (13)	8% (3)
Abdominal pain	71% (27)	68% (26)	47% (18)	18% (7)
Fatigue	66% (25)	26% (10)	61% (23)	3% (1)
Vomiting	66% (25)	58% (22)	18% (7)	3% (1)
Back pain	34% (13)	24% (9)	11% (4)	0
Anorexia	26% (10)	13% (5)	21% (8)	0
Edema limbs	18% (7)	0	18% (7)	0
Fever	18% (7)	11% (4)	11% (4)	0
Constipation	16% (6)	5% (2)	11% (4)	0
Dizziness	16% (6)	11% (4)	11% (4)	0
Allergic reaction	13% (5)	13% (5)	5% (2)	0
Arthralgia	13% (5)	3% (1)	11% (4)	0
Dyspnea	13% (5)	0	13% (5)	0
Shoulder pain	13% (5)	5% (2)	11% (4)	0
Ascites	11% (4)	0	11% (4)	3% (1)
Chills	11% (4)	0	11% (4)	0
Dysgeusia	11% (4)	3% (1)	11% (4)	0
Gastric stenosis	3% (1)	0	3% (1)	3% (1)
Hepatic failure*	3% (1)	0	3% (1)	3% (1)
Liver abscesses	3% (1)	0	3% (1)	3% (1)
Paroxysmal atrial tachycardia	3% (1)	0	3% (1)	3% (1)
Thoracic pain	3% (1)	3% (1)	3% (1)	3% (1)
Upper gastrointestinal hemorrhage	3% (1)	0	3% (1)	3% (1)

*We suspected mix of disease progression and radioembolization induced liver disease. This patient is also included in parameter "ascites."

Numbers of events are in parentheses. Adverse events are those with incidence of >10% or CTCAE grade 3 or 4, after treatment, regardless of relation with ^{166}Ho radioembolization.

The other patient, with rectal cancer, developed hepatic failure, for which expedited diagnostic studies showed intrahepatic and extrahepatic disease progression. Neither permitted autopsy.

Quality of Life

Quality of life was affected by ^{166}Ho radioembolization mostly in the short term (within 1 wk), after which it returned to baseline values. The median global health status decreased from 83 at baseline to 42 after 1 wk and recovered to 67 after 6 wk (interquartile ranges, 67–83, 25–71, and 56–83, respectively). The most affected functional scales were physical, role, and social functioning (Fig. 3A, all scores in Supplemental Table 1). The worst symptoms were comparable to the most common adverse events: fatigue, eating, pain, and emotional problems, all of which peaked after 1 wk (Fig. 3B).

Imaging

After treatment, recovered ^{166}Ho activity on SPECT/CT was slightly overestimated by a mean of 9.3% ± 7.1%. The scout dose of ^{166}Ho-microspheres was recovered, with a mean overestimation of 6.4% ± 6.0%. A median of 0.02% (range, 0%–0.7%) of the administered ^{166}Ho activity was present in the lungs after treatment. This percentage agreed with the median lung shunt after the scout dose of ^{166}Ho-microspheres: 0.01% (range, 0%–0.3%). After ^{99m}Tc-MAA injection, a median lung shunt of 3.2% (range, 0.01%–19.3%) was measured; no patients were excluded from treatment on the basis of their lung shunt.

Accuracy and precision were lower for MR quantification than for SPECT/CT, mainly because of unexpected noise in the images related to the adjusted acquisition parameters. On average, 51% ± 18% to 67% ± 17% (depending on the applied noise threshold) of all ^{166}Ho was recovered in the liver.

DISCUSSION

In this cohort of salvage patients with metastatic liver lesions, the target lesions of 73% of the patients showed disease control after 3 mo—an indicator of efficacy. For colorectal cancer patients, disease control in the liver was achieved in 45% after 3 mo, whereas reported disease control rates when applying best supportive care are around 10% (*20,21*).

The median survival of 13.4 mo (95% CI, 8.2–15.7 mo) in colorectal liver metastasis patients after treatment with ^{166}Ho-microspheres fits in the previously reported range of 8.3–15.2 mo after ^{90}Y radioembolization (*22*). In one of the few prospective

TABLE 5
Adverse Events—Laboratory Examinations

Adverse event	Grade 1–2	Grade 3	Grade 4	NA
γ-glutamyl transferase	6	28	4	0
Lymphocytopenia	15	6	1	0
Bilirubin	12	0	1	0
Alkaline phosphatase	32	6	0	0
Aspartate aminotransferase	35	3	0	0
Alanine aminotransferase	28	2	0	0
Lactate dehydrogenase	27	0	0	0
Hemoglobin	26	0	0	0
Ammonia	22	0	0	0
Albumin	20	0	0	0
Platelet count	19	0	0	0
Erythrocytes	15	0	0	0
Sodium	15	0	0	2
Leukocytes	14	0	0	0
Creatinine	12	0	0	0
Potassium	9	0	0	2
Total protein	9	0	0	4
Calcium (ionized)	8	0	0	3
Magnesium	6	0	0	4
Phosphorus	6	0	0	3
Urea	6	0	0	3
Chloride	5	0	0	4
Bicarbonate	4	0	0	4

NA = not available.
Maximum CTCAE grade of adverse event during follow-up after treatment is shown; some of these adverse events were preexistent.

studies on salvage patients treated with ^{90}Y-glass microspheres, Benson et al. (n = 61) reported a median overall survival of 8.8 mo (*23*).

Radioembolization with ^{166}Ho-microspheres was associated with several adverse events of grade 3 or higher, most of which were transient and manageable: abdominal pain and nausea were most common (18% and 8%, respectively). In the aforementioned prospective study by Benson et al., the rates of grade 3 or 4 adverse events were slightly lower than or comparable to the rates in this study, whereas fewer patients had abdominal pain in a retrospective cohort study by Kennedy et al.: the occurrence of grade 3 or 4 (abdominal) pain was 18% in this study versus 13% and 6% in the studies of Benson et al. and Kennedy et al., respectively, the occurrence of nausea 8% versus 1% and 1%, the occurrence of vomiting 3% versus 3% and 2%, and the occurrence of fatigue 3% versus 3% and 6% (*23,24*).

A strength of this study was the conservative analysis of efficacy; progressive disease was inferred if patients had missing data. And when there was disagreement between the 3 readers on the primary outcome, it was conservatively considered to be progressive disease.

A limitation of this study was that the 95% CIs for the primary outcome were not adjusted for the interim analysis because no valid methodology is known; the reported intervals were probably narrower than they should have been.

Personalized dosimetry can increase the efficacy of radioembolization. Garin et al. showed that ^{90}Y-microsphere treatment can safely be intensified in selected patients (based on pretreatment ^{99m}Tc-MAA dosimetry) (*4*). Patients with a higher absorbed dose (>205 Gy) to the tumors showed a longer time to progression. By combining pretreatment ^{99m}Tc-MAA and ^{99m}Tc-labeled sulfur colloid, Lam et al. were able to calculate both the absorbed dose to tumors and the absorbed dose to healthy liver parenchyma. These absorbed doses correlated with the response and toxicity, respectively (*2*).

An advantage of ^{166}Ho-microspheres over the commonly used ^{99m}Tc-MAA is that the absorbed dose to the lungs can be more accurately predicted with a scout dose (*6*). This is important, because the prescribed activity is reduced in up to 40% of patients (based on ^{99m}Tc-MAA) to reduce the probability of radiation pneumonitis (*25*). Furthermore, a scout dose using the same ^{166}Ho-microspheres is expected to predict the treatment-dose distribution (i.e., dosimetry) better than is possible with ^{99m}Tc-MAA (*26,27*). The presence of γ-emission does increase radiation exposure to some extent, but only patients treated with more than 7 GBq of ^{166}Ho and released within 6 h after treatment (instead of 24 h) would require contact restrictions. In all other cases, patients can be released without contact restrictions (*28*).

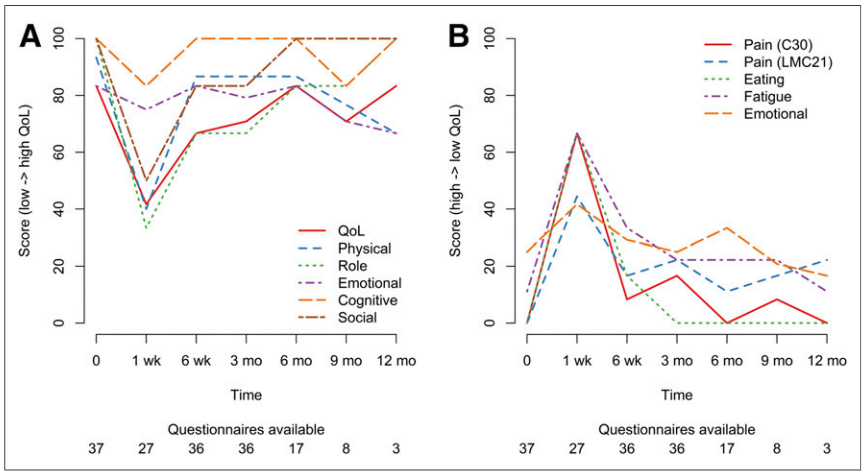

FIGURE 3. (A) Median quality-of-life (QoL) scores per time point (higher score = better QoL). (B) Median symptom scores per time point (higher score = worse symptoms).

CONCLUSION

This single-arm phase 2 study showed that radioembolization with ^{166}Ho-microspheres induced a response in salvage patients with metastatic liver malignancies.

DISCLOSURE

Marnix Lam is a consultant for BTG and Mirada. He received honoraria from Sirtex. Johannes Nijsen and Bernard Zonnenberg

are inventors on the patents related to the ^{166}Ho-microspheres; these patents are assigned to University Medical Center Utrecht Holding BV (patents US 6373068 B1 and US 2005/0201940 A1). Johannes Nijsen is cofounder and chief scientific officer (0.5FTE) of Quirem Medical BV and has a minority share in the company. He is inventor on the following U.S. patent families: 6373068 B1, 8632751, EP07112807.8, 10190254.2, and P112614NL00. Maarten Smits had accommodation expenses reimbursed by Quirem Medical BV. Bernard Zonnenberg received honoraria from GSK Netherlands, and he received honoria, consulted for, received research funding from, and had expenses reimbursed by Novartis Pharm Inc. Stavros Nikolakopoulos reports personal fees from Mapi Group consultancy, outside the submitted work. The Department of Radiology and Nuclear Medicine of the University Medical Center Utrecht receives royalties from Quirem Medical BV. This study was sponsored by a grant from the Dutch Cancer Society (KWF Kankerbestrijding), which had no role in the writing of the manuscript or the decision to submit it for publication. No other potential conflict of interest relevant to this article was reported.

ACKNOWLEDGMENTS

We acknowledge Tjitske Bosma, Otto Elgersma, Anneke Hamersma, Hugo de Jong, John de Klerk, Gerard Krijger, Gerrit van de Maat, Bastiaan van Nierop, Rob van Rooij, Remmert de Roos, Ingeborg van der Tweel, Frank Vleggaar, and Helena Verkooijen for their notable efforts in this study.

REFERENCES

1. Gates VL, Esmail AAH, Marshall K, Spies S, Salem R. Internal pair production of ^{90}Y permits hepatic localization of microspheres using routine PET: proof of concept. *J Nucl Med.* 2011;52:72–76.
2. Lam MGEH, Goris ML, Iagaru AH, Mittra ES, Louie JD, Sze DY. Prognostic utility of ^{90}Y radioembolization dosimetry based on fusion ^{99m}Tc-macroaggregated albumin-^{99m}Tc-sulfur colloid SPECT. *J Nucl Med.* 2013;54:2055–2061.
3. Chiesa C, Maccauro M, Romito R, et al. Need, feasibility and convenience of dosimetric treatment planning in liver selective internal radiation therapy with ^{90}Y microspheres: the experience of the National Tumor Institute of Milan. *Q J Nucl Med Mol Imaging.* 2011;55:168–197.
4. Garin E, Lenoir L, Edeline J, et al. Boosted selective internal radiation therapy with ^{90}Y-loaded glass microspheres (B-SIRT) for hepatocellular carcinoma patients: a new personalized promising concept. *Eur J Nucl Med Mol Imaging.* 2013;40:1057–1068.
5. Elschot M, Smits MLJ, Nijsen JFW, et al. Quantitative Monte Carlo-based holmium-166 SPECT reconstruction. *Med Phys.* 2013;40:112502.
6. Elschot M, Nijsen JFW, Lam MGEH, et al. ^{99m}Tc-MAA overestimates the absorbed dose to the lungs in radioembolization: a quantitative evaluation in patients treated with ^{166}Ho-microspheres. *Eur J Nucl Med Mol Imaging.* 2014;41:1965–1975.
7. Bourgeois AC, Chang TT, Bradley YC, Acuff SN, Pasciak AS. Intraprocedural yttrium-90 positron emission tomography/CT for treatment optimization of yttrium-90 radioembolization. *J Vasc Interv Radiol.* 2014;25:271–275.
8. Smits ML, Nijsen JF, van den Bosch MA, et al. Holmium-166 radioembolisation in patients with unresectable, chemorefractory liver metastases (HEPAR trial): a phase 1, dose-escalation study. *Lancet Oncol.* 2012;13:1025–1034.
9. Prince JF, Van Den Bosch MAAJ, Nijsen JFW, et al. Supplementary data: efficacy of radioembolization with holmium-166 microspheres in salvage patients with liver metastases: a phase 2 study. Zenodo website. https://zenodo.org/record/1169867. Published August 27, 2017. Accessed February 1, 2018.
10. Zielhuis SW, Nijsen JFW, de Roos R, et al. Production of GMP-grade radioactive holmium loaded poly(L-lactic acid) microspheres for clinical application. *Int J Pharm.* 2006;311:69–74.
11. Eisenhauer EA, Therasse P, Bogaerts J, et al. New response evaluation criteria in solid tumours: revised RECIST guideline (version 1.1). *Eur J Cancer.* 2009;45:228–247.
12. Sterne JAC, White IR, Carlin JB, et al. Multiple imputation for missing data in epidemiological and clinical research: potential and pitfalls. *BMJ.* 2009;338:b2393.
13. Common Terminology Criteria for Adverse Events (CTCAE): version 4.0. National Cancer Institute Enterprise Vocabulary Services website. http://evs.nci.nih.gov/ftp1/CTCAE/CTCAE_4.03_2010-06-14_QuickReference_5x7.pdf. Published May 28, 2009. Updated June 14, 2010 (version 4.03). Accessed February 1, 2018.
14. Bol GH, Kotte ANTJ, van der Heide UA, Lagendijk JJW. Simultaneous multimodality ROI delineation in clinical practice. *Comput Methods Programs Biomed.* 2009;96:133–140.
15. van de Maat GH, Seevinck PR, Elschot M, et al. MRI-based biodistribution assessment of holmium-166 poly(L-lactic acid) microspheres after radioembolisation. *Eur Radiol.* 2013;23:827–835.
16. van de Maat GH, de Leeuw H, Seevinck PR, van den Bosch MA, Nijsen JFW, Bakker CJG. Simultaneous R2*, R2, and R2′ quantification by combining S0 estimation of the free induction decay with a single spin echo: a single acquisition method for R2 insensitive quantification of holmium-166-loaded microspheres. *Magn Reson Med.* 2015;73:273–283.
17. Stallard N, Todd S. Exact sequential tests for single samples of discrete responses using spending functions. *Stat Med.* 2000;19:3051–3064.
18. Whitehead J. *The Design and Analysis of Sequential Clinical Trials.* New York, NY: John Wiley and Sons; 1997.
19. Agresti A, Coull BA. Approximate is better than "exact" for interval estimation of binomial proportions. *Am Stat.* 1998;52:119–126.
20. Van Cutsem E, Peeters M, Siena S, et al. Open-label phase III trial of panitumumab plus best supportive care compared with best supportive care alone in patients with chemotherapy-refractory metastatic colorectal cancer. *J Clin Oncol.* 2007;25:1658–1664.
21. Jonker DJ, O'Callaghan CJ, Karapetis CS, et al. Cetuximab for the treatment of colorectal cancer. *N Engl J Med.* 2007;357:2040–2048.
22. Rosenbaum CENM, Verkooijen HM, Lam MGEH, et al. Radioembolization for treatment of salvage patients with colorectal cancer liver metastases: a systematic review. *J Nucl Med.* 2013;54:1890–1895.
23. Benson AB, Geschwind J-F, Mulcahy MF, et al. Radioembolisation for liver metastases: results from a prospective 151 patient multi-institutional phase II study. *Eur J Cancer.* 2013;49:3122–3130.
24. Kennedy AS, Ball D, Cohen SJ, et al. Multicenter evaluation of the safety and efficacy of radioembolization in patients with unresectable colorectal liver metastases selected as candidates for ^{90}Y resin microspheres. *J Gastrointest Oncol.* 2015;6:134–142.
25. Gaba RC, Zivin SP, Dikopf MS, et al. Characteristics of primary and secondary hepatic malignancies associated with hepatopulmonary shunting. *Radiology.* 2014;271:602–612.
26. Wondergem M, Smits MLJ, Elschot M, et al. ^{99m}Tc-macroaggregated albumin poorly predicts the intrahepatic distribution of ^{90}Y resin microspheres in hepatic radioembolization. *J Nucl Med.* 2013;54:1294–1301.
27. Smits MLJ, Elschot M, Sze DY, et al. Radioembolization dosimetry: the road ahead. *Cardiovasc Intervent Radiol.* 2015;38:261–269.
28. Prince JF, Smits MLJ, Krijger GC, et al. Radiation emission from patients treated with holmium-166 radioembolization. *J Vasc Interv Radiol.* 2014;25:1956–1963.